I&EC research
Industrial & Engineering Chemistry Research

Article

pubs.acs.org/IECR

Magnetic Field-Induced Compressive Property of Magnetorheological Elastomer under High Strain Rate

Guojiang Liao, Xinglong Gong,* and Shouhu Xuan*

CAS Key Laboratory of Mechanical Behavior and Design of Materials, Department of Modern Mechanics, University of Science and Technology of China, Hefei 230027, China

ABSTRACT: The dynamic compressive property of magnetorheological elastomer (MRE) under high strain rate was investigated using a modified split Hopkinson pressure bar system. Both the compressive properties in the pre-yield region and the post-yield region were studied. Experimental results show that the dynamic compressive property of MRE under high strain rate is related to the magnetic field and the strain rate. In the pre-yield region, with increasing magnetic field or strain rate, both the Young's modulus and the yield stress increase. However, the yield strain decreases with increasing magnetic field or strain rate. A constitutive model consisting of hyperelasticity, viscoelasticity, and a magnetic part was proposed to describe the compressive property of MRE, and the model agrees well with the experimental results. In the post-yield region, the stress first decreases to a minimum value and then increases smoothly when the strain exceeds the yield strain, which is due to the change of the chainlike structures of iron particles in MRE.

1. INTRODUCTION

The experimental mechanical property of a material can be categorized into quasi-static property and dynamic property by the strain rate. When the strain rate is larger than 10^2/s, the mechanical property can be regarded as the dynamic property under high strain rate.[1,2] Typically, for the strain rate-sensitive material, such as elastomers and polymer foams, the dynamic property under high strain rate differs widely from the quasi-static property. These materials usually have a feature of low impedance, and a wide range of applications for shock-absorbing components has been found, such as engine mounts, gaskets, and so on.[3,4] When designing these components with low impedance materials, it is necessary to have accurate material models to predict the dynamic response of the structure. Therefore, the dynamic property under high strain rate is crucial. Reliable experimental data are useful to construct the material model and determine the material constants.

When traditional experimental techniques are used to measure the dynamic property under high strain rate of low impedance materials, problems occur.[4−9] For example, the rotating eccentric test machine can only be used to measure samples with large strain at relatively low frequencies; vibrating machines, such as the dynamic mechanical analysis machine (DMA), can measure the dynamic property at very high frequencies with sinusoidal or other waveform input but cannot achieve large strains; the dynamic destructive Charpy test can not provide a complete stress−strain history. To solve these problems, the split Hopkinson pressure bar (SHPB) can be considered. The SHPB technology can provide dynamic stress−strain curves as a function of strain rate in the range of strain rate from 10^2/s to 10^4/s. However, traditional SHPB technology can only be used to measure the dynamic property of hard materials, such as metal, concrete, ceramic, and so on. When this technology is directly used to measure the soft materials with the features of low strength and low mechanical impedance, some problems occur, such as low signal-to-noise ratio, long time to reach stress equilibrium, and so on. Recently, some researchers have investigated the SHPB technology thoroughly.[2−4,10,11] They proposed the use of a pulse shaper to prolong the rising time of the incident pulse and achieve the dynamic stress equilibrium of the specimen. In addition, they proved that a sensitive transmission bar and thin specimen were of benefit to obtain satisfying signal-to-noise ratio. Theses researchers did innovative studies and made it possible to investigate the dynamic property of low impedance materials in the range of strain rate from 10^2/s to 10^4/s.

Magnetorheological elastomer (MRE), also called magneto-sensitive elastomer, magneto-active polymer, or magneto-strictive polymer, is a kind of composite material consisting of micrometer-sized ferromagnetic particles embedded in rubber or a rubberlike matrix.[12−18] Its properties such as shear modulus, damping, magnetostriction, electrical, conductivity and so on, can be controlled by an external magnetic field, which is called magnetorheological effect (MR effect).[19−21] Due to the unique property, MRE has been widely used in vibration absorbers, isolators, engine mounts, bushing, actuators, etc.[22−29] Since MRE was first developed,[30] many studies have been carried out to investigate the magnetic field-induced properties and the corresponding mechanisms. Among all the magnetic field-induced properties of MRE, the shear property is of the most concern due to the relatively large change of the shear modulus when exposed to an external magnetic field. However, polymer-based materials can bear more loads in compressive status than in shear status.[6,31] When the MRE works in shear mode, it needs glues to connect the MRE samples and the shearing block, which limits the maximum deformation of MRE samples.[22,23] Therefore, it is proper for MRE to work in compressive status in the design of

Received: March 18, 2013
Revised: May 25, 2013
Accepted: May 30, 2013
Published: May 30, 2013

dx.doi.org/10.1021/ie400864d | *Ind. Eng. Chem. Res.* 2013, 52, 8445−8453

MRE-based devices when MRE needs to bear large loads. In addition, MRE is a material with low impedance and magnetic-field-controllable properties, allowing it to have potential application in controllable shock-absorbing components, such as engine mounts, gaskets, and so on.[3,4] When designing these components, it is necessary to know the compressive properties of MRE under high strain rate. However, up to now, the studies on the compressive property of MRE are limited and focus on the dynamic viscoelastic property.[5−7,32,33] For example, Kallio[5] studied the changes in the stiffness and vibration damping of MRE under the influence of a magnetic field when tested in dynamic compression. Koo[7] investigated the dynamic compression properties of MRE under cyclic loading and proposed a phenomenon model to explain the experimental results. These researchers did enlightening studies on the compressive property of MRE. However, more work needs to be done to evaluate the application of MRE. Therefore, study on the compressive property of MRE under high strain rate is very important.

In this work, the dynamic compressive property of MRE under high strain rate was studied using the modified split Hopkinson pressure bar technology. Both the dynamic compressive property in the pre-yield region and the post-yield region were investigated. A constitutive model consisting of hyperelasticity, viscoelasticity, and a magnetic part was proposed to describe the dynamic property of MRE, and the model agrees well with the experimental results. The study in this contribution will be useful to a deeper understanding of MRE and of benefit to the design of MRE-based devices.

2. EXPERIMENTAL DETAILS

2.1. Sample Preparation. The materials include carbonyl iron particles (Type CN, from BASF in Germany), methyl silicone oil (from Shanghai Resin Factory Co., Ltd.), HTV silicone rubber (Type MVQ 110-2, from Dong Jue Fine Chemicals Nanjing Co., Ltd.), and vulcanizing agent (double methyl double benzoyl hexane, from Shenzhen Gujia Company). The methyl silicone oil, viscosity 50 cP, was used as a plasticizer to improve the processing of rubber mixing. The mass ratio of the carbonyl iron particles to the others is 4:1. The procedure of fabricating MRE is as follows.

First, the HTV silicone rubber was subjected to heat treatment at 150 °C for 4 h to reduce the air bubbles in the rubber. Then, the rubber was placed in a double-roll mill (model XK-160, Taihu Rubber Machinery Inc., China) to be thoroughly mixed with carbonyl iron particles, vulcanizing agent, and silicone oil for roughly one hour. Later, the rubber mixture was used for vulcanizing MRE samples. Before vulcanizing, the rubber mixture was placed into an aluminum mold. Then the mold was fixed to a customized magnet−heat-coupled device (Figure 1). This device can supply a vertical magnetic field and keep the rubber mixture at a fixed temperature. The magnetic flux density in this process was roughly 1.5 T, and the temperature was 120 °C . This process lasted for 20 min. Then the mold with the rubber mixture was placed on a flat vulcanizer (model BL-6170-B, Bolon Precision Testing Machines Co., China,) for vulcanizing. The vulcanizing process was conducted at a temperature of 160 °C for 5 min. After that, the MRE samples were obtained.

2.2. Modified SHPB Technology for MRE. A typical split Hopkinson pressure bar (SHPB) system consists of a striker bar, an incident bar, a transmission bar, and an absorber bar, which is shown in Figure 2. The specimen is placed between

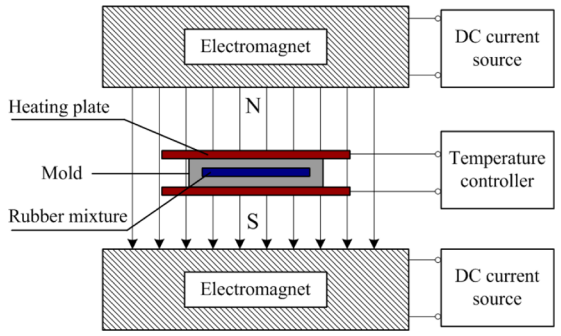

Figure 1. Sketch of customized magnet−heat-coupled device.

the incident bar and the transmission bar. Usually, the striker bar is driven by the gas produced by an air-compressor to hit the incident bar. The impact generates an elastic compressive wave at the impact face. The elastic compressive wave keeps on traveling in the incident bar toward the specimen. When the elastic compressive wave reaches the interface of the incident bar and the specimen, one part of the elastic compressive wave reflects into the incident bar, and the other part transmits into the specimen and into the transmission bar. Usually, two strain gauges are mounted on the incident bar and the transmission bar to measure the incident pulse (ε_i), the reflected pulse (ε_r), and the transmitted pulse (ε_t). According to the wave propagation theory in solids, the dynamic stress, the dynamic strain, and the strain rate at any time during the loading−unloading in the specimen can be expressed as:

$$\begin{cases} \sigma_s = \dfrac{E_b A_b}{A_s}\varepsilon_t \\ \varepsilon_s = -\dfrac{2C_b}{l_s}\displaystyle\int_0^t \varepsilon_r \, d\tau \\ \dot{\varepsilon}_s = -\dfrac{2C_b}{l_s}\varepsilon_r \end{cases} \quad (1)$$

where σ_s and ε_s are the dynamic stress and the dynamic strain in the specimen respectively; $\dot{(\ )}$ denotes (d/dt); A_b and A_s are the cross-sectional areas of the bar and the specimen, respectively; E_b is the elastic modulus of the bar material; C_b is the velocity of elastic wave propagation in the bar, and l_s is the length of the specimen. It needs to be mentioned that the calculations in eq 1 are based on the assumption that the specimen undergoes homogeneous deformation and the bars are made of the same material with the same cross-sectional area.

In this work, a modified SHPB system was developed to investigate the compressive property of MRE under high strain rate. To prevent the mechanical impedance mismatch of the bar and the MRE specimen, the striker bar, the incident bar, the transmission bar, and the absorber bar were made of aluminum for its low mechanical impedance. To improve the signal-to-noise ratio, the strain gauge in the transmission bar was chosen as a semiconductor strain gauge instead of a traditional metal one. To decrease the friction between the MRE specimen and the bar, petroleum jelly was used in the interface of the MRE specimen and the bar. In addition, a pulse shaper was used between the striker bar and the incident bar to prolong the rise time of the incident pulse. Therefore, the MRE specimen had enough time for stress to reach equilibrium during the experiment. In the study, the diameter of the aluminum bar

dx.doi.org/10.1021/ie400864d | Ind. Eng. Chem. Res. 2013, 52, 8445−8453

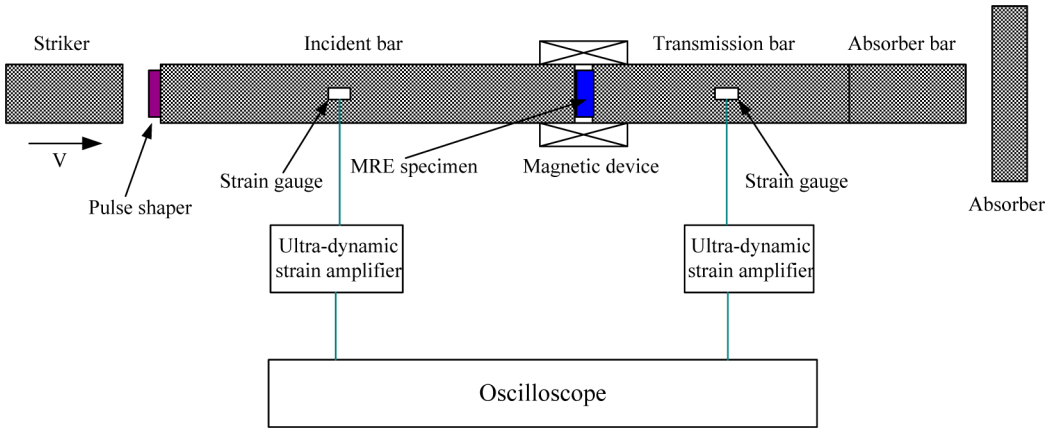

Figure 2. Schematic illustration of a modified SHPB setup.

was 14.5 mm, and the dimension of the MRE specimen was Φ8 mm × 1 mm. The length of the incident bar is 800 mm, and the length of the transmission bar is 600 mm. The model of the ultradynamic strain amplifier is CS-1D from Xingheng Electronic Technology Co., Ltd., China.

To investigate the compressive property of MRE under different external magnetic fields, a customized magnetic device was added into the SHPB system (Figure 2) to supply a uniform magnetic field. Figure 3a shows the schematic

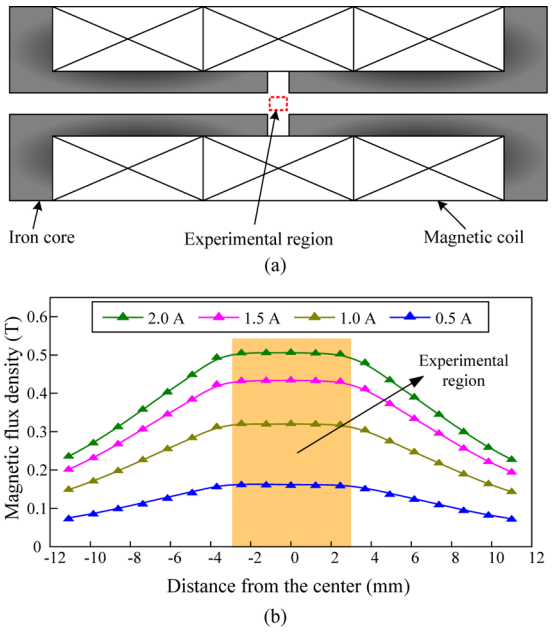

Figure 3. Schematic illustration of the customized magnetic device in the modified SHPB system: (a) sketch of the magnetic device; (b) magnetic flux density in the experimental region with different magnetic current.

illustration of the customized magnetic device. It consists of three magnetic coils and two iron cores. Figure 3b shows the magnetic field distribution in the experimental region along the symmetric axis under different magnetic currents. The experimental region lies in the center of the magnetic device and is about 6 mm along the symmetric axis. From the magnetic field distribution in Figure 3b, it can be seen that the magnetic field is constant in the whole experimental region and can be controlled by the magnetic current according to the demand. In addition, the length of the experimental region is about 6 mm, which is long enough to keep the MRE specimen in the experimental region during the loading−unloading process. In the experiment, the duration of loading−unloading is within 150 μs (Figure 4), and the maximal velocity of the

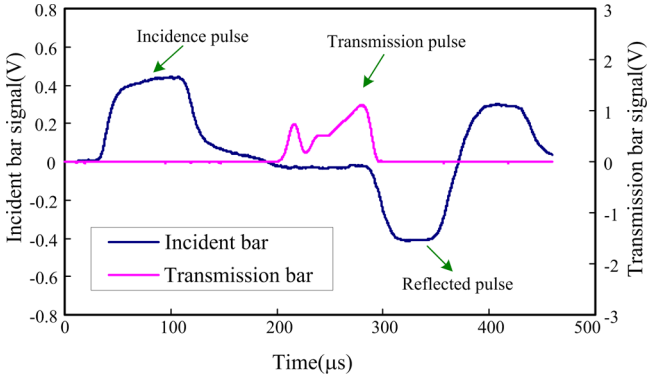

Figure 4. Typical signals measured from the incident bar and the transmission bar in the experiment.

striker bar is smaller than 30 m/s. According to the wave propagation theory in solids, the displacement of the interface between the MRE specimen and the incident bar is smaller than 2.25 mm. Therefore, the length of the experimental region is long enough to supply a uniform magnetic field to the MRE specimen during the loading−unloading process.

Figure 4 shows the typical signals measured by the strain gauges mounted on the incident bar and the transmission bar. Obviously, the signals are smooth enough, which means the signal-to-noise ratio is satisfying. In addition, it can be seen from Figure 4 that the rising edge of the incident pulse is gentle due to the pulse shaper, which guarantees that there is enough time for the MRE specimen to obtain stress equilibrium. Therefore, the experiment in the study is accurate. By reading the waveform in Figure 4 and using the formulas in eq 1, the magnetic field-induced stress−strain relationship of MRE under different strain rates can be obtained. In addition, the stress and the strain calculated from eq 1 are the engineering stress and engineering strain, respectively. The true stress and the true strain can be obtained from eq 2.

dx.doi.org/10.1021/ie400864d | Ind. Eng. Chem. Res. 2013, 52, 8445−8453

$$\begin{cases} \varepsilon_T = \ln(1 + \varepsilon_E) \\ \sigma_T = (1 + \varepsilon_E)\sigma_E \end{cases} \quad (2)$$

where ε_E and σ_E are the engineering strain and the engineering stress respectively, ε_T and σ_T are the true strain and the true stress, respectively.

3. RESULTS AND DISCUSSION

3.1. Compressive Property in the Pre-yield Region. The dynamic compressive property of MRE under different external magnetic fields and strain rates was measured. Figure 5

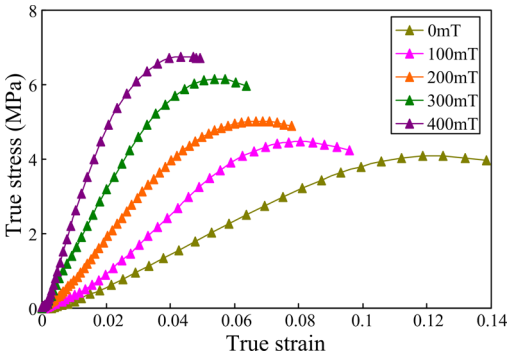

Figure 5. Dynamic compressive stress−strain curve of MRE at the average strain rate of 3200/s under different external magnetic fields.

shows the dynamic compressive stress−strain curve of MRE at the average strain rate of 3200/s under different magnetic fields in the pre-yield region. The strain and the stress in Figure 5 represent the true strain and the true stress, respectively. From Figure 5, it can be seen that the compressive property of MRE is dependent on the magnetic field. With increasing magnetic field, the stress−strain curve becomes steeper, which means the Young's modulus increases with increasing magnetic field. Similar to the shear property of MRE, the phenomenon that Young's modulus increases with increasing magnetic field can be named the MR effect, which results from the magnetic interactions between the iron particles under the external magnetic field.

For the polymer materials, the maximal stress and the corresponding strain during loading are defined as the yield stress and the yield strain, respectively. The stress−strain curve can be divided into two parts by the yield point, i.e. the pre-yield region and the post-yield region. Figure 5 shows the compressive property of MRE in the pre-yield region, and the property in the post-yield region will be discussed in the next section. Besides the Young's modulus increasing with the increasing magnetic field, another phenomenon is observed wherein the yield point is related to the external magnetic field. With increasing magnetic field, the yield stress increases and the yield strain decreases. The MRE consists of micrometer-sized ferromagnetic particles embedded in the matrix. The ferromagnetic particles form chain- or columnlike structures. With increasing external magnetic field, the magnetic interaction between the particles increases. Therefore, when the MRE specimen deforms in a larger external magnetic field, a larger force needs to be applied to overcome the magnetic force between the particles, which leads to the increase of the Young's modulus and the yield stress with the increasing external magnetic field. On the other hand, not only the magnetic interactions between the particles in the same chainlike structure but also the interactions between the particles in different chainlike structures increase when the magnetic field increases. Therefore, when the MRE specimen deforms, it is easer for the chainlike structure to be changed or broken in a higher magnetic field than in a lower magnetic field, which leads to the decreasing yield strain with increasing magnetic field. Figure 6 shows the dynamic compressive stress−strain curve of MRE at the strain rates of 4700/s and 5600/s under different external magnetic fields. Compared with the results in Figure 5, the stress−strain curves in Figure 6 show similar trends. Thus, a conclusion can be made from Figure 5 and Figure 6 that the dynamic compressive property of MRE under a high strain rate is dependent on the magnetic field. The Young's modulus and the yield stress increase with increasing magnetic field, and the yield strain decreases with increasing magnetic field.

In addition to the magnetic-field-dependent property, it is found that the compressive property of MRE is also related to the strain rate when comparing the results in Figure 5 with those in Figure 6. To show the results more clearly, the experimental data are rearranged and shown in Figure 7. For simplicity, only the results under 0 mT and 200 mT are shown in Figure 7 because the results under different magnetic fields are similar.

From Figure 7, the compressive property of MRE is related to the average strain rate. When the strain rate increases, the stress−strain curve becomes steeper, which means the Young's modulus increases with increasing strain rate. This phenomenon is also observed for other rubberlike materials and can be

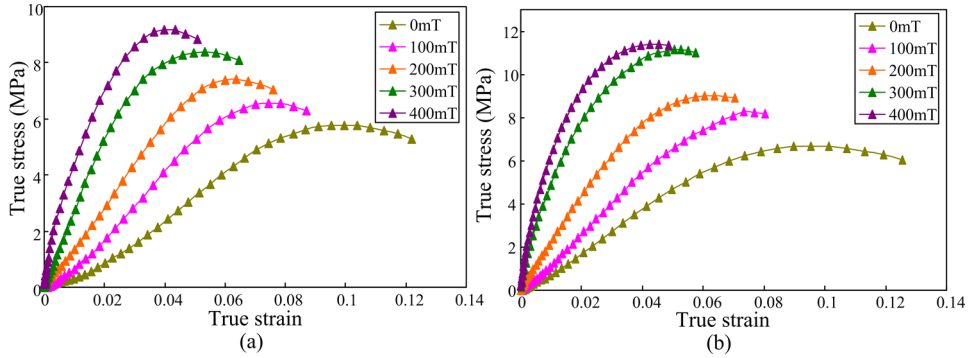

Figure 6. Dynamic compressive stress−strain curve of MRE at the average strain rate of (a) 4700/s and (b) 5600/s under different external magnetic fields.

dx.doi.org/10.1021/ie400864d | Ind. Eng. Chem. Res. 2013, 52, 8445−8453

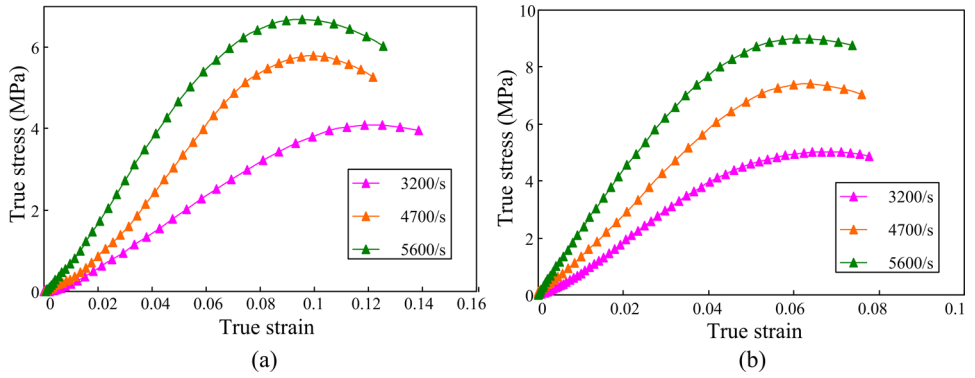

Figure 7. Dynamic compressive stress−strain curve of MRE at various strain rates under (a) 0 mT and (b) 200 mT.

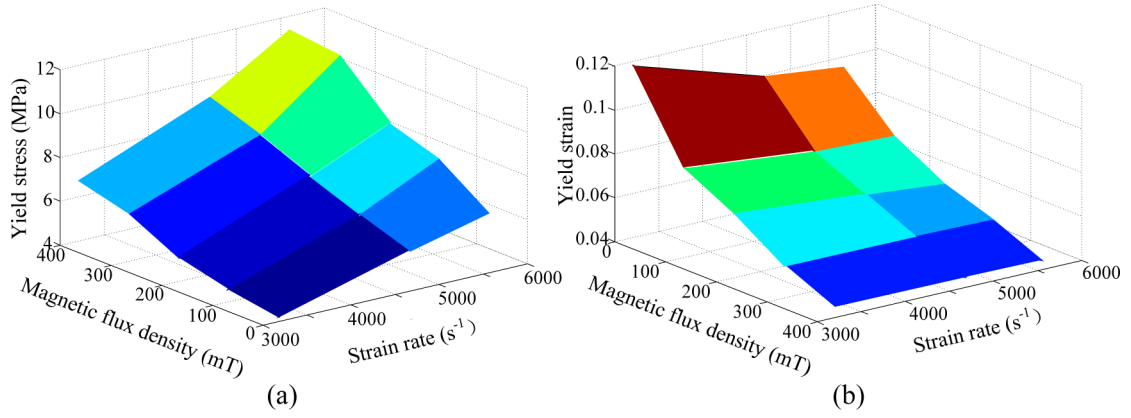

Figure 8. Yield stress (a) and yield strain (b) of MRE under different strain rates and different magnetic fields.

regarded as the typical property of this kind of material.[2,4,34,35] Besides the Young's modulus, the yield stress and the yield strain of MRE are also related to the strain rate. When the external magnetic field is 0 mT, the yield stress increases from 4.09 MPa at the strain rate of 3200/s to 6.68 MPa at the strain rate of 5600/s, while the yield strain decreases from 0.118 to 0.095. When the magnetic field is 200 mT, the yield stress increases from 5.02 MPa at the strain rate of 3200/s to 9.00 MPa at the strain rate of 5600/s, while the yield strain decreases from 0.068 to 0.060. Obviously, the yield stress increases with increasing strain rate. However, the yield strain decreases with increasing strain rate. To show the results more clearly, Figure 8 shows the yield stress and the yield strain of MRE under different strain rates and different magnetic fields. Thus, it can be summarized that when the strain rate increases, the MRE becomes stiffer and more brittle.

3.2. Constitutive Model of MRE in the Pre-yield Region. In order to describe the dynamic compressive property of MRE under high strain rate and facilitate the calculations in the engineering applications, a constitutive model is proposed on the basis of the strain-energy function method. MRE is a composite of polymer matrix and ferromagnetic particles. Therefore, it has the features of the polymer matrix and ferromagnetic particles. For the polymer matrix, it usually has the features of hyperelasticity and viscoelasticity. For the ferromagnetic particles, the typical property is the magnetic interactions among the particles, which leads to the magnetic-field-induced mechanical property of MRE. The proposed model in the study is a combination of hyperelasticity, viscoelasticity, and the magnetic part.

3.2.1. Hyperelasticity. The constitutive relation derived from a strain-energy function for uniaxial load can be expressed as[4,36]

$$\sigma_h = 2\left(\lambda^2 - \frac{1}{\lambda}\right)\left(\frac{\partial W}{\partial I_1} + \frac{1}{\lambda}\frac{\partial W}{\partial I_2}\right) \tag{3}$$

where W is the strain-energy function; I_1 and I_2 are the first and the second strain invariant, respectively; λ is the stretch ratio; and σ_h is the true stress. For the rubberlike materials, the strain−energy function under high strain rate can be written as[2,37]

$$W = A(I_1 - 3) + B(I_2 - 3) + C(I_1 - 3)(I_2 - 3) \tag{4}$$

where A, B, and C are material constants and determined through one dimension test. For the uniaxial compression, the stretch ratio, λ, can be written as:

$$\lambda = 1 - \varepsilon_e \tag{5}$$

where ε_e is the engineering strain. The first and the second strain invariant are

$$\begin{cases} I_1 = \lambda^2 + 2\lambda^{-1} \\ I_2 = \lambda^{-2} + 2\lambda \end{cases} \tag{6}$$

Therefore, by substituting eqs 4−6 into eq 3, the constitutive relation under uniaxial compression is written as

dx.doi.org/10.1021/ie400864d | Ind. Eng. Chem. Res. 2013, 52, 8445−8453

$$\sigma_h = 2\left[(1-\varepsilon_e)^2 - \frac{1}{1-\varepsilon_e}\right] \times \left\{A + \frac{B}{1-\varepsilon_e} + C\left[\frac{3}{(1-\varepsilon_e)^2} - \frac{3}{1-\varepsilon_e} - 3\varepsilon_e\right]\right\} \quad (7)$$

It needs to be mentioned that the strain in eq 7 is the engineering strain, and the stress represents the true stress.

3.2.2. Viscoelasticity. Polymer materials usually have the feature of viscoelasticity. To describe the viscoelasticity of MRE under high strain rate, a standard linear solid model shown in Figure 9 is adopted in the study. In Figure 9, E_1 and E_2 are the

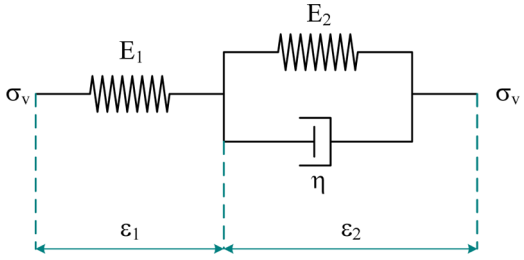

Figure 9. Standard linear solid model used to describe the viscoelasticity of MRE.

modulus of two spring elements respectively; η is the coefficient of viscosity; ε_1 and ε_2 are the strains of the two spring elements, respectively; σ_v is the stress. The constitutive equations of the model are written as

$$\sigma_v = E_1\varepsilon_1$$
$$\sigma_v = E_2\varepsilon_2 + \eta\dot{\varepsilon}_2$$
$$\varepsilon = \varepsilon_1 + \varepsilon_2 \quad (8)$$

Therefore, the stress−strain relation can be expressed as:

$$\eta\dot{\sigma}_v + (E_1 + E_2)\sigma_v = E_1\eta\dot{\varepsilon} + E_1E_2\varepsilon \quad (9)$$

Equation 9 can be transformed into

$$\dot{\sigma}_v + D\sigma_v = E\dot{\varepsilon} + F\varepsilon \quad (10)$$

where D, E, and F are the functions of the parameters shown in Figure 9 and determined by the material property. Solving eq 10 yields

$$\sigma_v = e^{-Dt}\int_0^t (E\dot{\varepsilon} + F\varepsilon)\, e^{D\xi}\, d\xi \quad (11)$$

3.2.3. Magnetic Part. The iron particles in MRE form chainlike structures. On the basis of the chainlike structures, Jolly[38] and Davis[39] proposed the magnetic dipole model to investigate the shear properties of MRE. Inspired by them, the magnetic dipole model is modified to investigate the magnetic field-induced compressive property in the study. Figure 10 shows the magnetic dipole model for MRE. It assumes that the iron particles are aligned in long chains and only the magnetic interactions between the particles within a chain are considered. The interaction energy of an iron particle marked i and the other particles within a chain can be expressed as

$$U = \frac{-1}{4\pi\mu_m\mu_0}\frac{4\zeta m^2}{d^3} \quad (12)$$

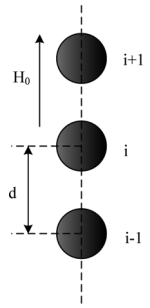

Figure 10. Magnetic dipole model for MRE.

where m is the magnetic dipole moment of the iron particle, μ_m is the relative permeability of the matrix, μ_0 is the permeability of vacuum, d is the distance of two adjacent particles, and ζ is a constant and can be expressed as

$$\zeta = \sum_{k=1}^{\infty}\frac{1}{k^3} \approx 1.202 \quad (13)$$

Then the magnetic energy density (energy per unit volume) can be written as

$$U_d = \frac{\phi}{2V}U \quad (14)$$

where V is the volume of a iron particle and ϕ is the volume fraction of the iron particles. The strain can be expressed as:

$$\varepsilon = \frac{d - d_0}{d_0} \quad (15)$$

where d_0 is the initial distance of two adjacent iron particles. Substituting eq 12 and 15 into eq 14 yields

$$U_d = \frac{-\phi}{2V\pi\mu_m\mu_0 {d_0}^3}\frac{\zeta m^2}{(1+\varepsilon)^3} \quad (16)$$

Then the magnetic field-induced stress can be expressed as

$$\sigma_m = \frac{\partial U_d}{\partial\varepsilon} = \frac{3\phi\zeta m^2}{2V\pi\mu_m\mu_0 {d_0}^3}\frac{1}{(1+\varepsilon)^4} = \frac{G}{(1+\varepsilon)^4} \quad (17)$$

where G is the function of the parameters shown in eq 17.

3.2.4. Total Stress. It is proposed that the total stress arises from a combination of the hyperelasticity, the viscoelasticity, and the magnetic part, i.e. $\sigma = \sigma_h + \sigma_v + \sigma_m$, where σ_h, σ_v, and σ_m are defined by eqs 7, 11 and 17, respectively.[2,34,35] Consequently, summation of eqs 7, 11 and 17 yields

$$\sigma = 2\left[(1-\varepsilon_e)^2 - \frac{1}{1-\varepsilon_e}\right] \times \left\{A + \frac{B}{1-\varepsilon_e} + C\left[\frac{3}{(1-\varepsilon_e)^2} - \frac{3}{1-\varepsilon_e} - 3\varepsilon_e\right]\right\} + e^{-Dt}\int_0^t (E\dot{\varepsilon} + F\varepsilon)\, e^{D\xi}\, d\xi + \frac{G}{(1+\varepsilon)^4} \quad (18)$$

where ε_e and ε are the engineering strain and the true strain, respectively; A, B, C, D, E, F, and G are the parameters to characterize the dynamic compressive property under high strain rate of MRE. Figure 11 shows the comparison between the experimental data and the fitted model. For simplicity, only the results at 0 mT and 200 mT are shown. The good

dx.doi.org/10.1021/ie400864d | Ind. Eng. Chem. Res. 2013, 52, 8445−8453

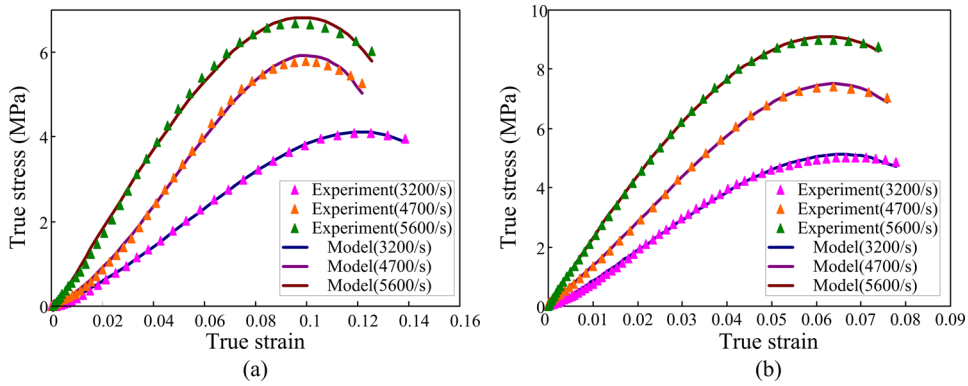

Figure 11. Comparison between the experimental data and the proposed model at (a) 0 mT and (b) 200 mT.

agreement between the experimental data and the proposed model indicates that the proposed model is capable of accurately describing the dynamic compressive property of MRE in the pre-yield region. Furthermore, the proposed constitutive model for MRE is efficient for numerical simulation in the design of MRE based devices.

3.3. Compressive Property in the Post-yield Region. To make a deeper understanding of MRE, the compressive property in the post-yield region was also investigated. Figure 12 shows the dynamic compressive stress−strain curve of MRE

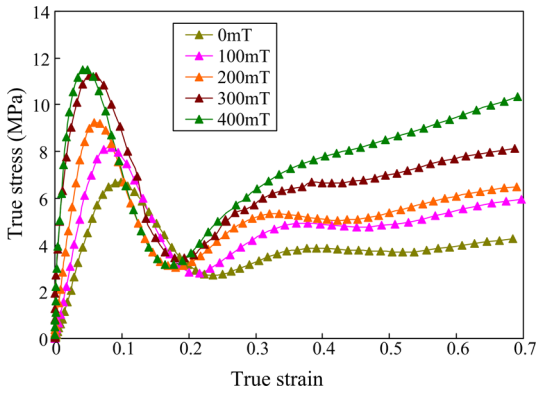

Figure 12. Dynamic compressive stress−strain curve of MRE at the strain rate of 5600/s under different external magnetic fields.

at the strain rate of 5600/s under different external magnetic fields. It can be seen that, when the strain exceeds the yield strain, the stress first decreases to a minimum value and then increases. This phenomenon is quite different from the rubberlike materials.[2,4,34,35] For the rubberlike materials, the yield strain is large. Therefore, the rubberlike materials always work in the pre-yield region, i.e. the stress increases with increasing strain in the experimental region. For the MRE, the yield strain is small. Therefore, once the strain exceeds the yield strain, the stress decreases. MRE is a composite of polymer matrix and ferromagnetic particles, which form chainlike structures. When subjected to impact load, these chainlike structures are easily broken due to the weak link between the particles and the matrix compared to the impact force. Thus, the yield strain of MRE is much smaller than the other rubberlike materials. When the strain exceeds the yield strain, the chainlike structures begin to break, and thus the stress decreases. With increasing compressive strain, MRE is further compressed and the distance between the iron particles becomes smaller and smaller. When the strain exceeds roughly 0.2, the distance between the iron particles becomes small enough, and thus, the stress begins to increase with increasing strain. Besides, in this region, it can be seen that the stress under higher magnetic field is larger than that under lower magnetic field, which is mainly due to the magnetic interaction between the iron particles.

Figure 13 shows the dynamic compressive property of MRE in the post-yield region at different strain rates. For simplicity, only the results under 0 mT and 200 mT are presented. It can be seen that the trends of the stress−strain curve are similar at different strain rates. However, obvious strain rate effect can also be observed, i.e. the stress at higher strain rate is larger than that at lower strain rate.

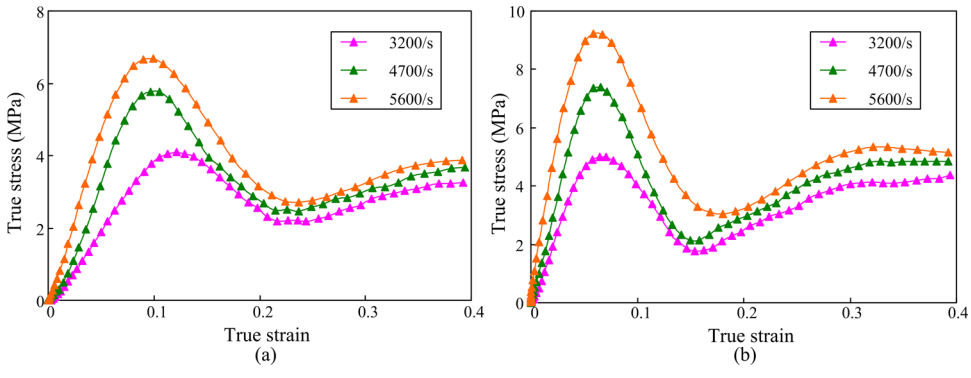

Figure 13. Dynamic compressive stress−strain curve of MRE at various strain rates under (a) 0mT and (b) 200 mT.

dx.doi.org/10.1021/ie400864d | Ind. Eng. Chem. Res. 2013, 52, 8445−8453

4. CONCLUSIONS

In this study, a modified SHPB system was used to investigate the dynamic compressive property of MRE under high strain rate. In the pre-yield region, it is found that both the yield stress and the Young's modulus increase with increasing magnetic field or strain rate, while the yield strain decreases. To describe the compressive property of MRE in the pre-yield region, a constitutive model consisting of hyperelasticity, viscoelasticity and magnetic part was proposed. The good agreement between the experimental data and the proposed model indicates that the proposed model is capable of accurately describing the dynamic compressive property of MRE in the pre-yield region. Beside the compressive property of MRE in the pre-yield region, the property in the post-yield region was also investigated. It is found that when the strain exceeds the yield strain, the stress first decreases to a minimum value and then increases. In addition, both the magnetic field effect and the strain rate effect were observed, i.e. the stress increases with increasing magnetic field or strain rate.

AUTHOR INFORMATION

Corresponding Author

*E-mail: gongxl@ustc.edu.cn (X.G.); xuansh@ustc.edu.cn (S.X.).

Notes

The authors declare no competing financial interest.

ACKNOWLEDGMENTS

Financial supports from the National Natural Science Foundation of China (Grant Nos. 11125210, 11072234, 11102202) and the National Basic Research Program of China (973 Program, Grant No. 2012CB937500) are gratefully acknowledged.

REFERENCES

(1) Stout, M. G.; Koss, D. A.; Liu, C.; Idasetima, J. Damage development in carbon/epoxy laminates under quasi-static and dynamic loading. *Compos. Sci. Technol.* **1999**, *59*, 2339.

(2) Xu, J.; Li, Y. B.; Ge, D. Y.; Liu, B. H.; Zhu, M. Y. Experimental investigation on constitutive behavior of PVB under impact loading. *Int. J. Impact Eng.* **2011**, *38*, 106.

(3) Chen, W.; Lu, F.; Frew, D. J.; Forrestal, M. J. Dynamic compression testing of soft materials. *J. Appl. Mech.* **2002**, *69*, 214.

(4) Song, B.; Chen, W. One-dimensional dynamic compressive behavior of EPDM rubber. *J. Eng. Mater. Technol.* **2003**, *125*, 294.

(5) Kallio, M.; Lindroos, T.; Aalto, S.; Jarvinen, E.; Karna, T.; Meinander, T. Dynamic compression testing of a tunable spring element consisting of a magnetorheological elastomer. *Smart Mater. Struct.* **2007**, *16*, 506.

(6) Liao, G. J.; Gong, X. L.; Xuan, S. H.; Guo, C. Y.; Zong, L. H. Magnetic-field-induced normal force of magnetorheological elastomer under compression status. *Ind. Eng. Chem. Res.* **2012**, *51*, 3322.

(7) Koo, J. H.; Khan, F.; Jang, D. D.; Jung, H. J. Dynamic characterization and modeling of magneto-rheological elastomers under compressive loadings. *J. Phys.: Conf. Ser.* **2009**, 012093.

(8) Harris, J. A. Dynamic testing under nonsinusoidal conditions and the consequences of nonlinearity for service performance. *Rubber Chem. Technol.* **1987**, *60*, 870.

(9) Clamroth, R. Determination of viscoelastic properties by dynamic testing. *Polym. Test* **1981**, *2*, 263.

(10) Lee, O. S.; Cho, K. S.; Kim, S. H.; Han, Y. H. Dynamic deformation behavior of soft material using SHPB technique and pulse shaper. *Int. J. Mod. Phys. B* **2006**, *20*, 3751.

(11) Song, B.; Chen, W. Dynamic compressive behavior of EPDM rubber under nearly uniaxial strain conditions. *J. Eng. Mater. Technol.* **2004**, *126*, 213.

(12) Bellan, C.; Bossis, G. Field dependence of viscoelastic properties of mr elastomers. *Int. J. Mod. Phys. B* **2002**, *16*, 2447.

(13) Gong, X. L.; Liao, G. J.; Xuan, S. H. Full-field deformation of magnetorheological elastomer under uniform magnetic field. *Appl. Phys. Lett.* **2012**, *100*, 211909.

(14) Tian, T. F.; Li, W. H.; Alici, G.; Du, H.; Deng, Y. M. Microstructure and magnetorheology of graphite-based MR elastomers. *Rheol. Acta* **2011**, *50*, 825.

(15) Ginder, J. M.; Clark, S. M.; Schlotter, W. F.; Nichols, M. E. Magnetostrictive phenomena in magnetorheological elastomers. *Int. J. Mod. Phys. B* **2002**, *16*, 2412.

(16) Li, W. H.; Zhang, X. Z. A study of the magnetorheological effect of bimodal particle-based magnetorheological elastomers. *Smart Mater. Struct.* **2010**, *19*, 035002.

(17) Liao, G. J.; Gong, X. L.; Xuan, S. H. Influence of shear deformation on the normal force of magnetorheological elastomer. *Mater. Lett.* **2013**, DOI: 10.1016/j.matlet.2013.05.035.

(18) Bica, I.; Balasoiu, M.; Kuklin, A. Anisotropic silicone rubber based magnetorheological elastomer with oil silicone and iron microparticles. *Solid State Phenom.* **2012**, *190*, 645.

(19) Mysore, P.; Wang, X. J.; Gordaninejad, F. Thick magneto-rheological elastomers. *Proc. SPIE - Int. Soc. Opt. Eng.* **2011**, DOI: 10.1117/12.881880.

(20) Li, W. H.; Zhou, Y.; Tian, T. F. Viscoelastic properties of MR elastomers under harmonic loading. *Rheol. Acta* **2010**, *49*, 733.

(21) Stolbov, O. V.; Raikher, Y. L.; Balasoiu, M. Modelling of magnetodipolar striction in soft magnetic elastomers. *Soft Matter* **2011**, *7*, 8484.

(22) Liao, G. J.; Gong, X. L.; Xuan, S. H.; Kang, C. J.; Zong, L. H. Development of a real-time tunable stiffness and damping vibration isolator based on magnetorheological elastomer. *J. Intell. Mater. Syst. Struct.* **2012**, *23*, 25.

(23) Liao, G. J.; Gong, X. L.; Kang, C. J.; Xuan, S. H. The design of an active-adaptive tuned vibration absorber based on magneto-rheological elastomer and its vibration attenuation performance. *Smart Mater. Struct.* **2011**, *20*, 075015.

(24) Du, H. P.; Li, W. H.; Zhang, N. Semi-active variable stiffness vibration control of vehicle seat suspension using an MR elastomer isolator. *Smart Mater. Struct.* **2011**, *20*, 105003.

(25) Hu, G. L.; Guo, M.; Li, W. H.; Du, H. P.; Alici, G. Experimental investigation of the vibration characteristics of a magnetorheological elastomer sandwich beam under non-homogeneous small magnetic fields. *Smart Mater. Struct.* **2011**, *20*, 127001.

(26) Wang, X. J.; Gordaninejad, F.; Calgar, M.; Yanming, L.; Sutrisno, J.; Fuchs, A. Sensing behavior of magnetorheological elastomers. *J. Mech. Des.* **2009**, 091004.

(27) Kim, Y. K.; Koo, J. H.; Kim, K. S.; Kim, S. H. Suppressing harmonic vibrations of a miniature cryogenic cooler using an adaptive tunable vibration absorber based on magneto-rheological elastomers. *Rev. Sci. Instrum.* **2011**, *82*, 035103.

(28) Li, W. H.; Zhang, X. Z.; Du, H. P. Development and simulation evaluation of a magnetorheological elastomer isolator for seat vibration control. *J. Intell. Mater. Syst. Struct.* **2012**, *23*, 1041.

(29) Bica, I. Magnetoresistor sensor with magnetorheological elastomers. *J. Ind. Eng. Chem.* **2011**, *17*, 83.

(30) Shiga, T.; Okada, A.; Kurauchi, T. Magnetoviscoelastic behavior of composite gels. *J. Appl. Polym. Sci.* **1995**, *58*, 787.

(31) Albanese, A. M.; Cunefare, K. A., Properties of a magneto-rheological semiactive vibration absorber In *Smart Structures and Materials 2003: Damping and Isolation*; Agnes, G. S.; Wang, K.-W.; , Eds.; Proceedings of SPIE: The International Society for Optical Engineering; SPIE: Bellingham, WA, 2003; p 36.

(32) Bica, I. Compressibility modulus and principal deformations in magneto-rheological elastomer: The effect of the magnetic field. *J. Ind. Eng. Chem.* **2009**, *15*, 773.

(33) Farshad, M.; Le Roux, M. Compression properties of magnetostrictive polymer composite gels. *Polym. Test* **2005**, *24*, 163.
(34) Shim, V. P. W.; Yang, L. M.; Lim, C. T.; Law, P. H. A visco-hyperelastic constitutive model to characterize both tensile and compressive behavior of rubber. *J. Appl. Polym. Sci.* **2004**, *92*, 523.
(35) Yang, L. M.; Shim, V. P. W.; Lim, C. T. A visco-hyperelastic approach to modelling the constitutive behaviour of rubber. *Int. J. Impact Eng.* **2000**, *24*, 545.
(36) Ward, I. M. *Mechanical Properties of Solid Polymers*, 2nd ed.; Wiley: New York, 1983.
(37) Brown, R. P. *Physical Testing of Rubber*, 3rd ed.; London: Chapman & Hall: New York, 1996.
(38) Jolly, M. R.; Carlson, J. D.; Munoz, B. C. A model of the behaviour of magnetorheological materials. *Smart Mater. Struct.* **1996**, *5*, 607.
(39) Davis, L. C. Model of magnetorheological elastomers. *J. Appl. Phys.* **1999**, *85*, 3348.